HHS Public Access

Author manuscript

Behav Brain Res. Author manuscript; available in PMC 2020 December 30.

Published in final edited form as:

Behav Brain Res. 2019 December 30; 376: 112214. doi:10.1016/j.bbr.2019.112214.

Visual feedback during motor performance is associated with increased complexity and adaptability of motor and neural output

Robin L. Shafer[a], **Eli Solomon**[b], **Karl M. Newell**[c], **Mark H. Lewis**[d], **James W. Bodfish**[a,e]

[a]Vanderbilt Brain Institute, Vanderbilt University, 6133 Medical Research Building III, 465 21st Avenue South, Nashville, TN, USA 37232.

[b]Neuroscience and Behavior Program, Wesleyan University Rm 257 Hall-Atwater, Wesleyan University, Middletown, CT 06459.

[c]Department of Kinesiology, University of Georgia, G3 Aderhold Hall, 110 Carlton Street, Athens, GA, USA 30602.

[d]Department of Psychiatry, University of Florida College of Medicine, PO Box 100256, L4-100 McKnight Brain Institute, 1149 Newell Drive, Gainesville, FL, USA 32611.

[e]Department of Hearing and Speech Sciences, Vanderbilt University Medical Center, 8310 Medical Center East, 1215 21st Avenue South, Nashville, TN, USA 37232

Abstract

Complex motor behavior is believed to be dependent on sensorimotor integration – the neural process of using sensory input to plan, guide, and correct movements. Previous studies have shown that the complexity of motor output is low when sensory feedback is withheld during precision motor tasks. However, much of this research has focused on motor behavior rather than neural processing, and therefore, has not specifically assessed the role of sensorimotor neural functioning in the execution of complex motor behavior. The present study uses a stimulus-tracking task with simultaneous electroencephalography (EEG) recording to assess the effect of visual feedback on motor performance, motor complexity, and sensorimotor neural processing in healthy adults. The complexity of the EEG signal was analyzed to capture the information content in frequency bands (alpha and beta) and scalp regions (central, parietal, and occipital) that are associated with sensorimotor processing. Consistent with previous literature, motor performance and its complexity were higher when visual feedback was provided relative to when it was withheld. The complexity of the neural signal was also higher when visual feedback was provided. This was most robust at frequency bands (alpha and beta) and scalp regions (parietal and occipital) associated with sensorimotor processing. The findings show that visual feedback increases the information available to the brain when generating complex, adaptive motor output.

Corresponding Author: Robin L. Shafer, robin.l.shafer@vanderbilt.edu, Vanderbilt Brain Institute, Vanderbilt University, 6133 Medical Research Building III, 465 21st Avenue South, Nashville, TN, USA 37232.

Keywords

entropy; sensorimotor integration; motor control; electroencephalography; autism; stereotypy

1 Introduction

The term complexity as has been frequently used to refer to physiologic signals that are highly variable and unpredictable [1–4] and has been operationally defined using various metrics including measures of entropy, spectral analysis, detrended fluctuation analysis, and Lempel-Ziv complexity [5,6]. High complexity is generally indicative of a healthy physiologic system as it signifies the ability of the system to integrate and respond adaptively to multiple sources of information about the ever-changing environmental conditions. The focus of the present study is to assess the effects of sensory feedback on the complexity of the neural and motor output during a sensorimotor task.

The influence of sensory feedback on the complexity of motor behavior has been demonstrated experimentally in children and adults through the manipulation of visual feedback during precision motor tasks (e.g., postural control or sustained grip force). These studies have found that when visual feedback is available, the motor output is more complex [7–10], implying a role for sensorimotor integration in the generation of complex and adaptive motor output. However, these studies have only evaluated motor behavior and have not assessed the neural mechanisms involved during these tasks.

Sensorimotor integration is the process through which the brain uses sensory information from the environment to plan and monitor movements, correct error in ongoing movements, and learn from previous motor experiences through feedforward and feedback processes [11–14]. These processes involve the translation of visual information in visual cortex to visuospatial information in posterior parietal cortex (PPC). PPC projects to frontal motor regions to generate the motor output. Cortico-pontinecerebellar circuitry is involved in comparing online visuospatial input from PPC with information about the motor command from motor cortex in order to monitor and correct motor error. There is also evidence that the basal ganglia are involved in the online generation and kinematic properties of corrective sub-movements [15,16].

As previously described, complex systems are those that integrate multiple sources of information to produce an adaptive output, which is often characterized by variability and unpredictability. The brain is an inherently complex system due to its highly integrative nature. As with other physiologic systems, measures of complexity (e.g. Multiscale Sample Entropy (MSE)) have been used to analyze the neural signal as a way to characterize brain function in disease states or experimental conditions [17–20]. The complexity of the neural signal has been shown to be positively associated with functional connectivity [21], and to relate to the level of information processing in the brain [20,22,23].

We recently proposed a conceptual model arguing that sensory feedback provides sensory systems with access to greater information, which is integrated into the motor system and used to generate a complex, adaptive motor output [24]. Consistent with the idea that more

complex motor behavior derives from a system with greater neural integration, studies of neural complexity across development have found age-related increases in neural complexity spanning from infancy to adulthood [25–27] that parallel the consistent increases in motor complexity that have been demonstrated in developmental studies of motor behavior [8–10,28].

In the present study, we use EEG metrics of neural complexity to assess how the presence and absence of visual feedback influences the processing of sensorimotor information during the production of precision movements. We hypothesize that access to visual feedback will produce a more complex neural signal and more complex and accurate movements.

2 Methods

2.1 Participants

Participants included 18 healthy, right-handed adults (10 females, 8 males) between the ages of 18 and 34 years (mean: 25.6 ± 4.9 years) with normal or corrected to normal vision. All participants were recruited from the Vanderbilt University and Vanderbilt University Medical Center communities and gave written informed consent to participate. This study was approved by the Vanderbilt University Institutional Review Board.

2.2 Equipment

Task stimuli were presented on a 24-inch high-definition (1920 × 1080 pixels) LCD computer monitor (ASUS VG248) from a PC (LG Electronics, Inc.) with 32GB of RAM at 4GHz. This PC was equipped with a NVIDIA GeForce GTX 770 graphics card and a dual monitor display. Participants used a wireless LED computer mouse to control the onscreen cursor during the sensorimotor task (described below). The sensorimotor task program was custom script programmed in MATLAB (The MathWorks, Inc., Natick, Massachusetts) using the Psychophysics Toolbox [29–31].

EEG data were collected using 128-electrode Electrical Geodesics, Inc (EGI) HydroCel Sensor Nets through EGI Net Station v.5 software on a Macintosh computer. The electrodes in the HydroCel Nets use a mild saline and shampoo solution. Electrodes were embedded in soft sponges and housed in pedestals.

2.3 Sensorimotor Task

Participants were seated in a dimly lit room, ~90cm in front of a 24-inch flat-screen computer monitor on which task instructions and stimuli were presented. Participants performed a stimulus-tracking task during which they controlled a cursor (green dot subtending a visual angle of ~0.3°) and followed a moving target (grey square subtending a visual angle of ~1°) that moved at a constant velocity of ~2°/s across the computer screen. The task consisted of two sensory conditions: (1) Visual feedback: participants saw the moving target and the cursor on the computer screen for the duration of the trial, (2) No visual feedback: the target and cursor were visible on the screen at the beginning of the trial, but disappeared mid-trial, and participants were instructed to continue moving the computer mouse as if the target and cursor were still visible. The target and cursor reappeared at the

end of the no visual feedback trials. The position of the cursor was sampled at 60Hz. The experiment consisted of eight experimental blocks, and each block consisted of 32 trials of a given sensory condition for a total of 256 trials (128 with visual feedback, 128 without visual feedback). The direction of target motion (up, down, left, right) was pseudo-randomized within a block, and all blocks contained 8 trials of each direction. The sensory feedback condition (with or without) alternated from one block to the next, and the condition of the first block was counterbalanced across participants. Figure 1 illustrates the task stimuli and experimental conditions.

Each block began with a set of instructions pertaining to the sensory feedback condition of the proceeding trials. Forced breaks were built in to the task to minimize participant fatigue. A 10s break occurred after every 8 trials, and a 2min break occurred at the end of each block (32 trials). To ensure that participants were attending to the trials, they were presented with the instructions and prompted to press the space bar to continue the task after each break. Additionally, participants were required to move the cursor into the target to initiate each trial. The delay between the moment the participant moved the cursor into the target and the moment the target started moving was randomized between 1.5 and 2.25s to minimize anticipatory movements.

2.4 EEG Data Collection and Processing

EEG data were collected in Net Station v.5 software continuously throughout the sensorimotor task. Data were sampled at 1000Hz and online referenced to the vertex electrode (corresponding to Cz in the International 10–20 system). The initiation and termination of the EEG recording, and the signaling of event triggers were controlled by custom MATLAB script on the stimulus PC via hard wired signals sent through the amplifier. Event triggers marked the moment during each trial in the sensorimotor task when the target and cursor disappeared (No Feedback trials) or the corresponding time point in the Feedback trials (~1.7s after the onset of target motion). EEG data were processed and cleaned in EEGLAB version 14.1.1b software [32] for MATLAB. Data were high pass filtered at 0.5 Hz and low pass filtered at 30 Hz and re-referenced to the average of all electrodes. Data were epoched from the window of −1s to 3.6s surrounding the moment during each trial when the target and cursor disappeared (No Feedback trials) or the corresponding time point in the Feedback trials. This epoch encompassed a baseline period of 1s of target movement while the target and cursor were present (consistent across both feedback conditions) and the entire segment of the trial when the conditions differed (target and cursor were not visible during the No Feedback trials but were visible during the Feedback trials).

Impedance of all electrodes was maintained below 50kΩ. Noisy and bad electrode channels were identified based on visual inspection and spherically interpolated. No more than 12/128 channels (~10%) per participant were interpolated. Eye blink artifact was identified using independent components analysis. Components related to blinks were identified based on strong frontal topography and punctate activation of the component, and these components were removed. For other types of artifact, epochs containing artifact were identified based on visual inspection and were removed. A minimum of 45 clean trials per condition was

required for the participant's data to be included in the analyses. Based on these criteria, none of the participants' data were excluded from the analyses. The number of trials retained did not differ significantly between the Feedback (mean: 81.78, standard deviation: 11.97) and No Feedback (mean: 74.78, standard deviation: 13.16) conditions.

2.5 Data Analysis

Participant movement was monitored through the position of the cursor on the screen. Only the data from the time the cursor and target disappeared to the time they reappeared (for the No Feedback trials) and the corresponding time segment from the Feedback trials were considered for the analyses as these represent the time segments during which the two conditions differed. Motor performance was analyzed according to two axes of movement: the axis of cursor movement that was parallel to the motion of the target, and the axis of cursor movement that was perpendicular to the motion of the target (e.g., if the target was moving rightward or leftward, parallel movements would be rightward or leftward movements made by the participant, and perpendicular movements would be upward and downward movements made by the participant). Error was calculated as the root mean squared error (RMSE) of the cursor position relative to the target position. The RMSE was calculated for each trial separately and then averaged across a participant for each condition and axis of motion such that each participant had two averaged RMSE values (parallel and perpendicular) for each feedback condition. All participants' average RMSE values were included as dependent variables in a 2×2 ANOVA with feedback condition (Feedback, No Feedback) and axis of motion (Parallel, Perpendicular) as independent repeated measures variables.

To verify that motor learning was not contributing to RMSE, we ran a repeated measures ANOVA for each sensory feedback condition to compare RMSE across blocks. Block number was the independent repeated measures variable. Each sensory feedback condition had 4 blocks. Participants' average RMSE across each block were the dependent variables.

Movement and neural complexity were assessed using entropy measures. Entropy measures were chosen as they are commonly used in studies of both motor [9,33–35] and neural [17,18,20,21,25] complexity. Additionally, sample entropy is relatively robust to short time series [36], allowing us to use short trial durations and limit the fatigue and time demands of the participants.

Movement complexity was assessed using the sample entropy (SampEn) [36,37] of the cursor position relative to the target over time. SampEn was calculated for each trial separately and then averaged across the participant for each condition and axis of motion such that each participant had two averaged SampEn values (parallel and perpendicular) for each feedback condition. All participants' average SampEn values were included as dependent variables in a 2×2 ANOVA with feedback condition and axis of motion as independent repeated measures variables.

SampEn(m, r, N) is a calculation of the self-similarity or regularity of a time series, and it is defined as the negative natural logarithm of the conditional probability that two similar sequences of m points in a data series of length N remain similar within a tolerance level of r

at the next point in the time series, where m is the embedding dimension, r is the tolerance, and N is the length of the data series [36,37]. Lower values of SampEn indicate greater self-similarity or regularity in the data series. SampEn is relatively robust to the length of the data series, and it has been shown to be reliable with data series as short as 200 data points.

To verify that motor learning was not contributing to SampEn, we ran a repeated measures ANOVA for each sensory feedback condition to compare SampEn across blocks. Block number was the independent repeated measures variable. Each sensory feedback condition had 4 blocks. Participants' average SampEn across each block were the dependent variables.

Neural complexity was assessed using multi-scale sample entropy (MSE) [3,4] of the time series of the EEG data. MSE is calculated as the SampEn at different time scales of the time series. The SampEn of the original time series is the value for scale one. For scale two, the original time series is essentially down sampled by averaging across every 2 consecutive data points in the series and then calculating the SampEn for the down sampled time series. Each subsequent scale down samples across increasing numbers of consecutive data points in the original time series and calculating SampEn for each of these down sampled time series. MSE can be represented as a curve of SampEn across scales, or the average value across all scales can be used as a general measure of complexity.

The MSE for the broad-spectrum EEG signal (0.5–30Hz) was calculated for each electrode on each trial separately and then averaged across electrodes and participant for each condition such that each participant had two sets of averaged MSE values – one for the Feedback condition and one for the No Feedback condition. The broad-spectrum data were analyzed using a 2×17 repeated measures ANOVA with feedback condition (Feedback vs. No Feedback) and time scale (1–17) as the independent factors. Regional MSE analyses were conducted on the specific frequency bands alpha/mu (8–13Hz; referred to hereafter simply as alpha) and beta (13–30Hz). MSE analyses on specific frequency bands have been done in previous studies [38,39]. Alpha and beta were selected due to the relevance of these frequency bands to sensorimotor processing [40–42]. Additionally, previous studies assessing motor-related neural complexity have looked specifically at complexity in these frequency bands [43,44].

For regional analyses, electrode clusters were defined according to scalp region and are described in relation to the 10–20 system. These included left and right frontal clusters centered around F3 and F4, respectively; left and right central clusters centered around C3 and C4, respectively; left and right parietal clusters centered around P3 and P4, respectively; left and right occipital clusters centered around O1 and O2, respectively; and left and right temporal clusters centered around T7 and T8, respectively. Frontal clusters were chosen based on their likelihood of capturing a signal relevant to executive functioning. Central and parietal clusters were chosen based on their likelihood of capturing a motor relevant signal. Occipital clusters were chosen based on their likelihood of capturing a visually relevant signal, and the temporal clusters were chosen as control regions, as these scalp regions are unlikely to capture task-relevant activity. MSE values for each cluster were calculated per participant per condition as the average MSE values across trials of all electrodes in the cluster. Regional data were analyzed according to region and feedback condition for each

time scale. Additionally, the average MSE values across time scales were calculated for each region and condition. These averaged MSE values were included as the dependent variable in a 2 × 5 × 2 repeated measures ANOVA with feedback condition (Feedback, No Feedback), region (Frontal, Central, Parietal, Occipital, Temporal), and laterality (Left, Right) as the independent variables.

For whole scalp analyses, MSE values were calculated per participant as the average across trials within a condition and across all electrodes on the scalp. Whole scalp data were analyzed according to condition for each time scale. Additionally, the average MSE values across time scales were calculated for each condition, and a Tukey test was used to analyze differences in feedback conditions for these averaged values.

To relate the motor complexity findings to the neural complexity findings, correlational analyses between the motor complexity data and the neural complexity data were run for each participant and feedback condition. For this analysis, the broad-spectrum EEG data were down-sampled to 60Hz to match the sampling rate of the motor data. MSE was calculated on the down-sampled EEG, and the MSE values were averaged across time scales and electrodes for each participant. Within each feedback condition and participant, the motor complexity and the neural complexity were correlated across trials. Slope and fit were averaged across participants for each feedback condition. Only the motor data corresponding to the parallel axis of motion were used, since this axis had the greatest variability.

3 Results

3.1 Motor Performance

The results of the 2×2 rmANOVA with feedback condition (Feedback, No Feedback) and axis of motion (Perpendicular, Parallel) as independent variables are summarized in Figure 2. This analysis revealed a significant main effect of feedback condition driven by greater RMSE in the No Feedback condition compared to the Feedback condition ($F(1,17)=210.25$, $p<0.001$, $\eta_p^2 = 0.925$), a significant main effect of axis of motion driven by greater RMSE in the Parallel axis than in the Perpendicular axis ($F(1,17)=11.04$, $p=0.004$, $\eta_p^2 = 0.394$), and a significant feedback condition x axis of motion interaction ($F(1,17)=9.96$, $p=0.006$, $\eta_p^2 = 0.370$). Follow-up analyses revealed that RMSE was greater in the No Feedback condition than the Feedback condition for both the Parallel ($F(1,17)=76.11$, $p<0.001$, $\eta_p^2=0.817$) and Perpendicular ($F(1,17)=65.74$, $p<0.001$, $\eta_p^2=0.795$) axes of movement; however, the magnitude of the differences between sensory feedback conditions was significantly greater in the Parallel axis than the Perpendicular axis ($t(17)=3.16$, $p=0.006$, $d=1.229$).

The rmANOVAs used to assess learning effects on RMSE, with block number as the independent variable, did not find differences in RMSE across blocks for the Feedback or the No Feedback condition.

3.2 Motor Complexity

The results of the 2×2 rmANOVA with feedback condition and axis of motion as independent variables are summarized in Figure 3. This analysis revealed a significant main effect of feedback condition driven by greater SampEn in the Feedback condition relative to

the No Feedback Condition ($F(1,17)=779.25$, $p<0.001$, $\eta_p^2 = 0.979$), a significant main effect of axis of motion driven by greater SampEn in the Parallel axis of motion than in the Perpendicular axis ($F(1,17)=564.1$, $p<0.001$, $\eta_p^2 = 0.971$), and a significant feedback condition x axis of motion interaction ($F(1,17)=690.63$, $p<0.001$, $\eta_p^2 = 0.976$). Follow-up analyses revealed the SampEn was greater in the Feedback condition than the No Feedback condition for both the Parallel ($F(1,17)=762.22$, $p<0.001$, $\eta_p^2=0.978$) and Perpendicular ($F(1,17)=301.46$, $p<0.001$, $\eta_p^2=0.947$) axes of movement; however the magnitude of the differences between sensory feedback conditions was significantly greater in the Parallel axis than the Perpendicular axis ($t(17)=26.28$, $p<0.001$, $d=7.843$).

The rmANOVAs used to assess learning effects on SampEn, with block number as the independent variable did not find differences in SampEn across blocks for the or the No Feedback condition.

3.3 Neural Complexity

Results of the ANOVA with feedback condition and time scale as independent variables revealed a significant main effect of sensory feedback condition ($F(1,17)=7.75$, $p=0.013$, $\eta_p^2=0.313$), a main effect of time scale ($F(1.55,17)=3642.60$, $p<0.001$, $\eta_p^2=0.995$), and a sensory feedback condition by time scale interaction ($F(1.234,17)=10.11$, $p=0.003$, $\eta_p^2=0.373$). The main effect of sensory feedback condition was driven by the Feedback condition having higher complexity than the No Feedback condition. Results are depicted in Figure 4. Differences that remained significant after correcting for multiple comparisons using Least Squares Difference are reported.

The results of the alpha ANOVA including scalp region and laterality as independent variables revealed significant main effects of feedback condition ($F(1,17) = 15.83$, $p = 0.001$, $\eta_p^2=0.482$), laterality ($F(1,17) = 4.92$, $p = 0.040$, $\eta_p^2= 0.224$), and region ($F(2.28, 17)$, $p < 0.001$, $\eta_p^2 = 0.522$). The main effect of feedback condition was driven by greater MSE in the Feedback condition. The main effect of laterality was driven by greater MSE in the Left hemisphere. The main effect of cluster was driven by lower MSE in the occipital region than in all other regions (Frontal: $t(17) = 5.53$, $p < 0.001$, $d = 1.30$; Central: $t(17) = 4.83$, $p < 0.001$, $d = 1.11$; Parietal: $t(17) = 3.85$, $p = 0.001$, $d = 0.907$; Temporal: $t(17) = 5.29$, $p < 0.001$, $d = 1.25$) and greater MSE in the temporal region than in Central ($t(17) = 2.82$, $p < 0.001$, $d = 0.665$) and Parietal ($t(17) = 4.71$, $p < 0.001$, $d = 1.11$) regions.

There were significant interactions between feedback condition and region ($F(1.50, 17) = 14.99$, $p < 0.001$, $\eta_p^2= 0.469$) and laterality and region ($F(2.09, 17) = 3.69$, $p = 0.033$, $\eta_p^2= 0.178$). Follow-up comparisons revealed that the feedback condition by region was driven by the strongest reduction in MSE in the occipital region in the No Feedback condition relative to the Feedback condition. Follow-up comparisons revealed that the laterality by region interaction was driven by greater MSE in the left hemisphere for the Parietal ($t(17) = 2.36$, $p = 0.030$, $d = 0.557$) and Occipital ($t(17) = 2.13$, $p = 0.047$, $d = 0.504$) regions only. Results for the alpha frequency band analyses are depicted in Figure 5. Condition differences at each scale that remained significant after correcting for multiple comparisons using Least Significant Difference are indicated.

Results of the beta ANOVA including scalp region and laterality revealed a significant main effect of feedback condition ($F(1,17) = 8.66$, $p = 0.009$, $\eta_p^2 = 0.338$). Follow-up analyses revealed that this main effect was driven by greater MSE in the Feedback condition. No other main effects were significant. There was a significant interaction between feedback condition and region ($F(1.86, 17) = 5.18$, $p = 0.013$, $\eta_p^2 = 0.234$). Follow-up analyses revealed that this interaction was driven by higher MSE in the Feedback condition for the Central ($t(17) = 2.43$, $p = 0.026$, $d = 0.573$), Parietal ($t(17) = 3.73$, $p = 0.002$, $d = 0.880$), Occipital ($t(17) = 2.63$, $p = 0.018$, $d = 0.620$), and Temporal ($t(17) = 2.34$, $p = 0.032$, $d = 0.551$) regions, but not the Frontal region. No other interactions were significant. Results for the beta frequency band analyses are depicted in Figure 6. Condition differences at each scale that remained significant after correcting for multiple comparisons using Least Significant Difference are indicated.

3.4 Relation of Motor and Neural Complexity

For the correlations between motor complexity (SampEn) and neural complexity (overall MSE) for the Feedback condition, the slopes of the trend lines for individual participants ranged from −1.06 to 1.05, and R^2 values ranged from 0.00062 to 0.048 with an average slope of 0.078 and average R^2 of 0.013. For the No Feedback condition, slopes ranged from −0.43 to 0.78 and R^2 values ranged from 0.000078 to 0.050 with an average slope of 0.029 and average R^2 of 0.010. Indicating no significant relation between motor and neural complexity at the group level for either condition. These data are depicted in Figure 7.

4 Discussion

Visual feedback has repeatedly been shown to increase the complexity of motor output on precision motor tasks [7–10,45,46]. Though these studies have been limited to assessing the effect of visual feedback on motor behavior, it is assumed that visual feedback increases the complexity of precision motor behavior through sensorimotor integration. In the present study, we examined the role of sensorimotor integration in the use of visual feedback to increase motor complexity by measuring the effect of visual feedback on the complexity of the EEG signal during a precision motor task. Importantly, we replicated previous findings that motor complexity increases and motor error decreases when visual feedback is provided during precision movement tasks [7–10,45,46]. We did not find evidence of learning effects in motor performance or motor complexity. Consistent with our hypotheses, we found that the complexity of the neural signal was elevated when visual feedback was available compared to when it was not. Additionally, the increased neural complexity when visual feedback was available paralleled the increase in motor complexity and decrease in motor error. Our results support that visual feedback influences motor complexity by increasing the information available to the brain, which uses the information to produce a more complex, adaptive motor output.

We observed significantly greater motor error and significantly lower motor complexity in the axis of movement parallel to the motion of the cursor compared to the perpendicular axis. The perpendicular axis had less variability of movement than the parallel axis, which could contribute to the differences in error and complexity.

4.1 Localized Effects of Visual Feedback on Neural Complexity

Based on our hypotheses of how the availability of sensory information influences the motor output, we expected both the visual-related (occipital) and the motor-related (central and parietal) neural signal to be higher in complexity when visual feedback was available compared to when it was not. Given that all participants were right-handed and used their right hand to perform the task, we expected a motor-related signal located centrally and parietally in the contralateral (left) hemisphere to the movement, as has been observed in previous studies of motor and visuomotor related cortical potentials and frequency-based analyses of motor processing [47–50].

For both the alpha and beta frequencies, we observed feedback related increases in neural complexity in the occipital scalp regions indicating, as hypothesized, that access to visual feedback increases the information available to and processed by visual cortex. Our results for both the alpha and beta frequency bands also revealed significantly greater complexity in left parietal regions compared to right parietal regions – consistent with a motor signal [47–50]. Left parietal regions also showed an effect of feedback, expressing significantly greater complexity when visual feedback was available compared to when it was not. These findings are in line with extant literature implicating parietal cortex in visuomotor processing. Parietal cortex is involved in visuospatial transformations [13,14,51], error monitoring [52], and online error correction [53] during visuomotor behavior.

We also observed increased neural complexity in the central scalp regions for both the alpha and beta analyses; however, neither of these analyses indicated an effect of laterality, so it is not clear whether these signals correspond to motor activity. The neural findings in occipital and left parietal scalp regions, combined with the motor performance and complexity findings support that when visual feedback is available, the visual system has access to more information, which is integrated into the motor system to produce a complex, adaptive motor output consistent with our conceptual model [24].

Of note, the alpha frequency band analyses revealed Feedback related increases in neural complexity in all scalp regions and increased neural complexity in the left occipital region in addition to the left parietal region. Similarly, the beta band analyses revealed feedback related increases in temporal scalp regions in addition to the motor and visually relevant regions. The distributed task related activity in the alpha frequency band is not surprising, as alpha has been associated with visual processing and attention in addition to sensorimotor processing [54,55]. Another possibility is that the temporal activity is associated with spatial memory; however, EEG studies of visual spatial memory generally observe task-relevant activity at frontal and parietal scalp regions rather than temporal regions [56,57]. The effects of laterality in the left occipital region for the alpha analyses and the effect of feedback on temporal regions could also be related to the poor spatial resolution inherent in EEG. It is possible the spread of the motor-related signal is being captured in the analyses of these neighboring regions.

In the alpha frequency analyses, we also observed increased neural complexity in the frontal scalp regions when visual feedback was available. This could be related to differences in error monitoring – when visual feedback is available, participants are able to assess errors in

their movements online (i.e., they can see when the cursor deviates from the target); however, when visual feedback is not available, participants are not able to monitor the accuracy of their movement to know when they are making errors. Frontal alpha has been found to be associated with error monitoring for errors that were not self-generated [58]. Frontal scalp localization of error processing has been repeatedly found in event related potential (ERP) studies that assess the error related negativity in various paradigms [59]. Additionally, Arrighi and colleagues [60] observed modulation of frontal (Fz) theta band activity that was time-locked to motor errors and event related spectral perturbations that were time locked to corrective movements when participants had visual feedback of their hand position during a reach-to-target task. These findings suggest that the differences in the effect of visual feedback on neural complexity at frontal electrode sites may be related to the processing of, and response to, errors that occur during the Feedback condition. Future studies should assess the effects of error processing on neural complexity.

4.2 Dynamical Complexity in the Brain

A truly complex biologic system, like the brain, needs to be adaptable across multiple time scales; therefore, complexity in the system should be high across multiple time scales [3,4]. To analyze our EEG data, we used multiscale sample entropy to assess the complexity of the neural system across multiple time scales. We found that for both sensory feedback conditions, the neural signal demonstrated high complexity across multiple time scales. We also observed that in the presence of visual feedback, neural complexity was higher across several time scales, in particular in scalp regions and frequency ranges associated with visual and motor processing, indicating that access to visual feedback enhances information processing in the sensorimotor system, permitting the system to produce more complex, adaptive behavior.

4.3 Implications for Typical Development and Clinical Disorders

The long-term goal of our research is to examine the role of sensorimotor integration deficits in neurodevelopmental disorders. Specifically, we are interested in how such deficits impact the development of the motor system and the clinical presentation of these disorders. It is first necessary, however, to understand the sensorimotor mechanisms that support the development of complex motor behavior in typically developing individuals. Stereotyped – rhythmic, repetitive – behavior occurs early in healthy infant development and is believed to serve as a foundation on which complex, adaptive motor behavior is built [61,62].

Motor complexity increases over the course of development; however, its expression is dependent on access to sensory input. Infant stereotypy decreases with greater amounts of sensory input (e.g., rocking, swinging, bouncing, and exploring) [63]. Additionally, a developmental increase in motor complexity is evident when visual feedback is provided during precision motor tasks; however, when visual feedback is withheld, all age groups display low complexity [8–10], implying that sensorimotor integration plays a role in the generation of complex and adaptive motor output.

Several neurodevelopmental, neuropsychiatric and neurodegenerative disorders present with sensorimotor disturbances including Parkinson’s Disease [64,65], schizophrenia [66,67], and

autism spectrum disorders (ASD) [68–70]. Studies have also found evidence of low motor complexity in these disorders [33–35,71]. Repetitive behavior including including punding in Parkinson's disease [72] and stereotyped behavior in schizophrenia [73], and ASD [74,75] is also common. Together these findings suggest that sensorimotor integration deficits may be contributing to the low motor complexity that has been observed in these clinical conditions.

We recently proposed that low complexity, repetitive behavior manifests as a result of poor sensorimotor integration [24]. In our healthy adult sample, we found that we could induce both high and low motor complexity by manipulating the availability of visual feedback during the motor task. This is consistent with findings that motor complexity is task dependent (i.e., there are tasks for which low motor complexity is optimal and tasks for which high motor complexity is optimal) [76]. What may distinguish the low motor complexity that we observed in healthy, mature individuals from that in healthy infants and clinical populations is the fact that healthy, mature individuals have malleable motor complexity – they are able to reliably integrate sensory information when it is available and use it to access more biomechanical degrees of freedom to generate more complex, adaptive movements. Whereas, infants, who have had limited sensory and motor experience and whose brains are immature may be limited to simple, stereotyped motor behavior [28,61,63], and low complexity, repetitive behavior in clinical populations could result from deficits in the sensorimotor neural circuitry that limits the adaptability of the motor output. This is supported by a recent study that found that although typically developing children showed increased motor complexity when visual feedback was available during a postural sway task, children with ASD demonstrated low motor complexity both in the presence and absence of visual feedback, indicating that the children with ASD were not integrating the visual information to support their motor control [68].

Understanding the role that sensorimotor integration plays in the expression of low motor complexity in clinical populations could aid in the development of treatments for improving adaptive behavior by targeting sensorimotor integration.

4.4 Limitations

Our study used EEG to assess neural activity associated with sensorimotor integration. EEG has notoriously poor spatial resolution; therefore, we cannot be certain that the task related activity we attributed to sensorimotor integration is originating from brain regions known to be involved in sensorimotor integration. Future research could use functional magnetic resonance imaging during the stimulus-tracking task to identify the involvement of specific brain regions during the task.

We did not observe a correlation between the motor complexity and neural complexity measures. This could be attributed to the fact that neural complexity was assessed using multiscale sample entropy, whereas, motor complexity was assessed using a single scale of sample entropy. The neural complexity values used for the correlations were the average sample entropy across time scales; therefore, they do not correspond to the timescale of the motor complexity data. We were not able to assess sample entropy at multiple time scales for the motor data due to the limited sampling rate of our equipment. Future studies will use

equipment with a high sampling rate to collect motor data. Additionally, other analytic approaches, including coherence, or within trial analyses such as wavelet coherence, may be more sensitive to the coupling between the neural and behavioral signals. These approaches should be considered for future studies.

Our results support previous findings that visual feedback increases motor complexity. It is important to note, however, that optimal physiologic complexity is task and condition dependent [76]. For motor behavior, there are task and environmental conditions for which reducing motor complexity is beneficial. For example, if the pattern of the target motion were sinusoidal as opposed to linear, the optimal motor pattern would likely be lower in complexity, limiting the effect of visual feedback on motor complexity. Neural complexity has been shown both to increase [77] and decrease [78] with increasing task difficulty indicating that the neural requirements involved in different tasks may differentially effect neural complexity.

5 Conclusions

Our study aimed to determine the role that sensorimotor integration plays in the expression of, complex motor patterns in typical adults through manipulating access to visual feedback during a motor task. Withholding visual feedback from participants resulted in poorer motor performance, lower motor complexity, and lower neural complexity, specifically in signals associated with sensorimotor integration. Our results suggest that sensorimotor integration permits the nervous system to use visual feedback to inform the motor system allowing it to generate adaptive motor output through online monitoring and correction of movements. When visual feedback is withheld, there is limited information for the brain to use to monitor the accuracy of the movement and generate adaptive motor corrections. This results in less complex and less accurate motor behavior. Our findings have implications for understanding and treating disorders such as ASD that present with low motor complexity and sensorimotor integration deficits.

Acknowledgements

Funding: This work was supported by the National Institutes of Health R01 HD082127 and U54HD083211; and the Vanderbilt Institute for Clinical and Translational Research VR51549.

Glossary

EEG	Electroencephalography
RMSE	Root mean squared error
SampEn	Sample entropy
MSE	Multiscale sample entropy
rmANOVA	Repeated measures analysis of variance
ASD	Autism spectrum disorder
FB	Feedback

NoFB No Feedback

References

[1]. Goldberger AL, Non-linear dynamics for clinicians: chaos theory, fractals, and complexity at the bedside, The Lancet. 347 (1996) 1312–1314. doi:10.1016/S0140-6736(96)90948-4.

[2]. Lipsitz LA, Goldberger AL, Loss of “Complexity” and Aging: Potential Applications of Fractals and Chaos Theory to Senescence, JAMA. 267 (1992) 1806–1809. doi:10.1001/jama.1992.03480130122036. [PubMed: 1482430]

[3]. Costa M, Goldberger AL, Peng C-K, Multiscale entropy analysis of biological signals, Phys. Rev. E 71 (2005). doi:10.1103/PhysRevE.71.021906.

[4]. Costa M, Goldberger AL, Peng C-K, Multiscale Entropy Analysis of Complex Physiologic Time Series, Phys. Rev. Lett 89 (2002). doi:10.1103/PhysRevLett.89.068102.

[5]. Aboy M, Hornero R, Abasolo D, Alvarez D, Interpretation of the Lempel-Ziv Complexity Measure in the Context of Biomedical Signal Analysis, IEEE Trans. Biomed. Eng 53 (2006) 2282–2288. doi:10.1109/TBME.2006.883696. [PubMed: 17073334]

[6]. Seely AJ, Macklem PT, Complex systems and the technology of variability analysis, Crit. Care 8 (2004) R367. doi:10.1186/cc2948. [PubMed: 15566580]

[7]. Athreya DN, Van Orden G, Riley MA, Feedback about isometric force production yields more random variations, Neurosci. Lett 513 (2012) 37–41. doi:10.1016/j.neulet.2012.02.002. [PubMed: 22342910]

[8]. Deutsch KM, Newell KM, Age Differences in Noise and Variability of Isometric Force Production, J. Exp. Child Psychol 80 (2001) 392–408. doi:10.1006/jecp.2001.2642. [PubMed: 11689037]

[9]. Deutsch KM, Newell KM, Children’s coordination of force output in a pinch grip task, Dev. Psychobiol 41 (2002) 253–264. doi:10.1002/dev.10051. [PubMed: 12325140]

[10]. Deutsch KM, Newell KM, Deterministic and stochastic processes in children’s isometric force variability, Dev. Psychobiol 43 (2003) 335–345. doi:10.1002/dev.10140. [PubMed: 15027417]

[11]. Desmurget M, Grafton S, Forward modeling allows feedback control for fast reaching movements, Trends Cogn. Sci 4 (2000) 423–431. doi:10.1016/S1364-6613(00)01537-0. [PubMed: 11058820]

[12]. Vaillancourt DE, Thulborn KR, Corcos DM, Neural Basis for the Processes That Underlie Visually Guided and Internally Guided Force Control in Humans, J. Neurophysiol 90 (2003) 3330–3340. doi:10.1152/jn.00394.2003. [PubMed: 12840082]

[13]. Ellermann JM, Siegal JD, Strupp JP, Ebner TJ, Ugurbil K, Activation of Visuomotor Systems during Visually Guided Movements: A Functional MRI Study, J. Magn. Reson 131 (1998) 272–285. doi:10.1006/jmre.1998.1379. [PubMed: 9571103]

[14]. Johnson PB, Ferraina S, Bianchi L, Caminiti R, Cortical networks for visual reaching: physiological and anatomical organization of frontal and parietal lobe arm regions, Cereb. Cortex 6 (1996) 102–119. [PubMed: 8670643]

[15]. Spraker MB, Yu H, Corcos DM, Vaillancourt DE, Role of Individual Basal Ganglia Nuclei in Force Amplitude Generation, J. Neurophysiol 98 (2007) 821–834. doi:10.1152/jn.00239.2007. [PubMed: 17567775]

[16]. Grafton ST, Tunik E, Human Basal Ganglia and the Dynamic Control of Force during On-Line Corrections, J. Neurosci 31 (2011) 1600–1605. doi:10.1523/JNEUROSCI.3301-10.2011. [PubMed: 21289168]

[17]. Ahmed MU, Li L, Cao J, Mandic DP, Multivariate multiscale entropy for brain consciousness analysis, in: 2011 Annu. Int. Conf. IEEE Eng. Med. Biol. Soc, IEEE, 2011: pp. 810–813. http://ieeexplore.ieee.org/xpls/abs_all.jsp?arnumber=6090185 (accessed June 24, 2016).

[18]. Catarino A, Churches O, Baron-Cohen S, Andrade A, Ring H, Atypical EEG complexity in autism spectrum conditions: A multiscale entropy analysis, Clin. Neurophysiol 122 (2011) 2375–2383. doi:10.1016/j.clinph.2011.05.004. [PubMed: 21641861]

[19]. Wang J, Noh G-J, Choi B-M, Ku S-W, Joo P, Jung W-S, Kim S, Lee H, Suppressed neural complexity during ketamine- and propofol-induced unconsciousness, Neurosci. Lett 653 (2017) 320–325. doi:10.1016/j.neulet.2017.05.045. [PubMed: 28572032]

[20]. Yang AC, Wang S-J, Lai K-L, Tsai C-F, Yang C-H, Hwang J-P, Lo M-T, Huang NE, Peng C-K, Fuh J-L, Cognitive and neuropsychiatric correlates of EEG dynamic complexity in patients with Alzheimer's disease, Prog. Neuropsychopharmacol. Biol. Psychiatry 47 (2013) 52–61. doi: 10.1016/j.pnpbp.2013.07.022. [PubMed: 23954738]

[21]. Wang DJJ, Jann K, Fan C, Qiao Y, Zang Y-F, Lu H, Yang Y, Neurophysiological Basis of Multi-Scale Entropy of Brain Complexity and Its Relationship With Functional Connectivity, Front. Neurosci 12 (2018). doi:10.3389/fnins.2018.00352.

[22]. Mizuno T, Takahashi T, Cho RY, Kikuchi M, Murata T, Takahashi K, Wada Y, Assessment of EEG dynamical complexity in Alzheimer's disease using multiscale entropy, Clin. Neurophysiol 121 (2010) 1438–1446. doi:10.1016/j.clinph.2010.03.025. [PubMed: 20400371]

[23]. Wu D, Cai G, Yuan Y, Liu L, Li G, Song W, Wang M, Application of nonlinear dynamics analysis in assessing unconsciousness: A preliminary study, Clin. Neurophysiol 122 (2011) 490–498. doi:10.1016/j.clinph.2010.05.036. [PubMed: 20719560]

[24]. Shafer RL, Newell KM, Lewis MH, Bodfish JW, A Cohesive Framework for Motor Stereotypy in Typical and Atypical Development: The Role of Sensorimotor Integration, Front. Integr. Neurosci 11 (2017). doi:10.3389/fnint.2017.00019.

[25]. Hasegawa C, Takahashi T, Yoshimura Y, Nobukawa S, Ikeda T, Saito DN, Kumazaki H, Minabe Y, Kikuchi M, Developmental Trajectory of Infant Brain Signal Variability: A Longitudinal Pilot Study, Front. Neurosci 12 (2018). doi:10.3389/fnins.2018.00566.

[26]. Lee GMH, Fattinger S, Mouthon A-L, Noirhomme Q, Huber R, Electroencephalogram approximate entropy influenced by both age and sleep, Front. Neuroinformatics 7 (2013). doi: 10.3389/fninf.2013.00033.

[27]. Miskovic V, Owens M, Kuntzelman K, Gibb BE, Charting moment-to-moment brain signal variability from early to late childhood, Cortex. 83 (2016) 51–61. doi:10.1016/j.cortex. 2016.07.006. [PubMed: 27479615]

[28]. Thelen E, Rhythmical stereotypies in normal human infants, Anim. Behav 27 (1979) 699–715. [PubMed: 556122]

[29]. Brainard DH, The Psychophysics Toolbox, Spat. Vis 10 (1997) 433–436. [PubMed: 9176952]

[30]. Kleiner M, Brainard DH, Pelli DG, What's new in Psychtoolbox-3?, Perception. 36 (2007) ECVP Abstract Supplement.

[31]. Pelli DG, The VideoToolbox software for visual psychophysics: Transforming numbers into movies, Spat. Vis 10 (1997) 437–442. [PubMed: 9176953]

[32]. Delorme A, Makeig S, EEGLAB: an open source toolbox for analysis of single-trial EEG dynamics including independent component analysis, J. Neurosci. Methods 134 (2004) 9–21. doi:10.1016/j.jneumeth.2003.10.009. [PubMed: 15102499]

[33]. Fournier KA, Amano S, Radonovich KJ, Bleser TM, Hass CJ, Decreased dynamical complexity during quiet stance in children with Autism Spectrum Disorders, Gait Posture. 39 (2014) 420–423. doi:10.1016/j.gaitpost.2013.08.016. [PubMed: 24055002]

[34]. Vaillancourt DE, Slifkin AB, Newell KM, Regularity of force tremor in Parkinson's disease, Clin. Neurophysiol 112 (2001) 1594–1603. [PubMed: 11514241]

[35]. Newell KM, Bodfish JW, Dynamical origins of stereotypy: Relation of postural movements during sitting to stereotyped movements during body-rocking, Am. J. Ment. Retard 112 (2007) 66–75. [PubMed: 17181392]

[36]. Yentes JM, Hunt N, Schmid KK, Kaipust JP, McGrath D, Stergiou N, The Appropriate Use of Approximate Entropy and Sample Entropy with Short Data Sets, Ann. Biomed. Eng 41 (2013) 349–365. doi:10.1007/s10439-012-0668-3. [PubMed: 23064819]

[37]. Richman JS, Moorman JR, Physiological time-series analysis using approximate entropy and sample entropy, Am. J. Physiol.-Heart Circ. Physiol 278 (2000) H2039–H2049. [PubMed: 10843903]

[38]. Ghanbari Y, Bloy L, Christopher Edgar J, Blaskey L, Verma R, Roberts TPL, Joint Analysis of Band-Specific Functional Connectivity and Signal Complexity in Autism, J. Autism Dev. Disord 45 (2015) 444–460. doi:10.1007/s10803-013-1915-7. [PubMed: 23963593]

[39]. Mišić B, Mills T, Taylor MJ, McIntosh AR, Brain Noise Is Task Dependent and Region Specific, J. Neurophysiol 104 (2010) 2667–2676. doi:10.1152/jn.00648.2010. [PubMed: 20844116]

[40]. Lin C-L, Shaw F-Z, Young K-Y, Lin C-T, Jung T-P, EEG correlates of haptic feedback in a visuomotor tracking task, NeuroImage. 60 (2012) 2258–2273. doi:10.1016/j.neuroimage.2012.02.008. [PubMed: 22348883]

[41]. McFarland DJ, Miner LA, Vaughan TM, Wolpaw JR, Mu and beta rhythm topographies during motor imagery and actual movements, Brain Topogr. N. Y 12 (2000) 177–86.

[42]. Mizuhara H, Cortical dynamics of human scalp EEG origins in a visually guided motor execution, NeuroImage. 62 (2012) 1884–1895. doi:10.1016/j.neuroimage.2012.05.072. [PubMed: 22659479]

[43]. Gao L, Wang J, Chen L, Event-related desynchronization and synchronization quantification in motor-related EEG by Kolmogorov entropy, J. Neural Eng 10 (2013) 036023. doi:10.1088/1741-2560/10/3/036023. [PubMed: 23676901]

[44]. Martínez-Vargas JD, Castro-Hoyos C, Castellanos-Dominguez G, Entropy-based multichannel measure of stationarity for characterization of motor imagery patterns, in: 2014 36th Annu. Int. Conf. IEEE Eng. Med. Biol. Soc, 2014: pp. 1469–1472. doi:10.1109/EMBC.2014.6943878.

[45]. Slifkin AB, Vaillancourt DE, Newell KM, Intermittency in the Control of Continuous Force Production, J. Neurophysiol 84 (2000) 1708–1718. doi:10.1152/jn.2000.84.4.1708. [PubMed: 11024063]

[46]. Vaillancourt DE, Russell DM, Temporal capacity of short-term visuomotor memory in continuous force production, Exp. Brain Res 145 (2002) 275–285. doi:10.1007/s00221-002-1081-1. [PubMed: 12136377]

[47]. Cespón J, Galdo - Álvarez S, Díaz F, Age-related changes in ERP correlates of visuospatial and motor processes, Psychophysiology. 50 (2013) 743–757. doi:10.1111/psyp.12063. [PubMed: 23730815]

[48]. Duann J-R, Chiou J-C, A Comparison of Independent Event-Related Desynchronization Responses in Motor-Related Brain Areas to Movement Execution, Movement Imagery, and Movement Observation, PLOS ONE. 11 (2016) e0162546. doi:10.1371/journal.pone.0162546. [PubMed: 27636359]

[49]. Naranjo JR, Brovelli A, Longo R, Budai R, Kristeva R, Battaglini PP, EEG dynamics of the frontoparietal network during reaching preparation in humans, NeuroImage. 34 (2007) 1673–1682. doi:10.1016/j.neuroimage.2006.07.049. [PubMed: 17196399]

[50]. Veldman MP, Maurits NM, Nijland MAM, Wolters NE, Mizelle JC, Hortobágyi T, Spectral and temporal electroencephalography measures reveal distinct neural networks for the acquisition, consolidation, and interlimb transfer of motor skills in healthy young adults, Clin. Neurophysiol 129 (2018) 419–430. doi:10.1016/j.clinph.2017.12.003. [PubMed: 29304417]

[51]. Buneo CA, Jarvis MR, Batista AP, Andersen RA, Direct visuomotor transformations for reaching, Nature. 416 (2002) 632–636. doi:10.1038/416632a. [PubMed: 11948351]

[52]. Grafton ST, Schmitt P, Van Horn J, Diedrichsen J, Neural substrates of visuomotor learning based on improved feedback control and prediction, NeuroImage. 39 (2008) 1383–1395. doi:10.1016/j.neuroimage.2007.09.062. [PubMed: 18032069]

[53]. Desmurget M, Epstein CM, Turner RS, Prablanc C, Alexander GE, Grafton ST, Role of the posterior parietal cortex in updating reaching movements to a visual target, Nat. Neurosci 2 (1999) 563–567. doi:10.1038/9219. [PubMed: 10448222]

[54]. Foster JJ, Sutterer DW, Serences JT, Vogel EK, Awh E, Alpha-Band Oscillations Enable Spatially and Temporally Resolved Tracking of Covert Spatial Attention, Psychol. Sci 28 (2017) 929–941. doi:10.1177/0956797617699167. [PubMed: 28537480]

[55]. Lobier M, Palva JM, Palva S, High-alpha band synchronization across frontal, parietal and visual cortex mediates behavioral and neuronal effects of visuospatial attention, NeuroImage. 165 (2018) 222–237. doi:10.1016/j.neuroimage.2017.10.044. [PubMed: 29074278]

[56]. Blacker KJ, Ikkai A, Lakshmanan BM, Ewen JB, Courtney SM, The role of alpha oscillations in deriving and maintaining spatial relations in working memory, Cogn. Affect. Behav. Neurosci 16 (2016) 888–901. doi:10.3758/s13415-016-0439-y. [PubMed: 27299431]

[57]. Smyrnis N, Protopapa F, Tsoukas E, Balogh A, Siettos CI, Evdokimidis I, Amplitude spectrum EEG signal evidence for the dissociation of motor and perceptual spatial working memory in the human brain, Exp. Brain Res 232 (2014) 659–673. doi:10.1007/s00221-013-3774-z. [PubMed: 24281356]

[58]. Zhang H, Chavarriaga R, del R Millán J, Discriminant brain connectivity patterns of performance monitoring at average and single-trial levels, NeuroImage. 120 (2015) 64–74. doi:10.1016/j.neuroimage.2015.07.012. [PubMed: 26169320]

[59]. Weinberg A, Dieterich R, Riesel A, Error-related brain activity in the age of RDoC: A review of the literature, Int. J. Psychophysiol 98 (2015) 276–299. doi:10.1016/j.ijpsycho.2015.02.029. [PubMed: 25746725]

[60]. Arrighi P, Bonfiglio L, Minichilli F, Cantore N, Carboncini MC, Piccotti E, Rossi B, Andre P, EEG Theta Dynamics within Frontal and Parietal Cortices for Error Processing during Reaching Movements in a Prism Adaptation Study Altering Visuo-Motor Predictive Planning, PLOS ONE. 11 (2016) e0150265. doi:10.1371/journal.pone.0150265. [PubMed: 26963919]

[61]. Konczak J, Borutta M, Topka H, Dichgans J, The development of goal-directed reaching in infants: hand trajectory formation and joint torque control, Exp. Brain Res 106 (1995) 156–168. [PubMed: 8542971]

[62]. Thelen E, Cooke DW, Relationship between newborn stepping and later walking: A new interpretation, Dev. Med. Child Neurol 29 (1987) 380–393. [PubMed: 3596074]

[63]. Thelen E, Determinants of amount of stereotyped behavior in normal human infants, Ethol. Sociobiol 1 (1980) 141–150.

[64]. Almeida QJ, Frank JS, Roy EA, Jenkins ME, Spaulding S, Patla AE, Jog MS, An evaluation of sensorimotor integration during locomotion toward a target in Parkinson's disease, Neuroscience. 134 (2005) 283–293. doi:10.1016/j.neuroscience.2005.02.050. [PubMed: 15950389]

[65]. Vaillancourt DE, Slifkin AB, Newell KM, Intermittency in the visual control of force in Parkinson's disease, Exp. Brain Res 138 (2001) 118–127. doi:10.1007/s002210100699. [PubMed: 11374078]

[66]. Kaufmann T, Skåtun KC, Alnæs D, Doan NT, Duff EP, Tønnesen S, Roussos E, Ueland T, Aminoff SR, Lagerberg TV, Agartz I, Melle IS, Smith SM, Andreassen OA, Westlye LT, Disintegration of Sensorimotor Brain Networks in Schizophrenia, Schizophr. Bull 41 (2015) 1326–1335. doi:10.1093/schbul/sbv060. [PubMed: 25943122]

[67]. Lencer R, Reilly JL, Harris MS, Sprenger A, Keshavan MS, Sweeney JA, Sensorimotor Transformation Deficits for Smooth Pursuit in First-Episode Affective Psychoses and Schizophrenia, Biol. Psychiatry 67 (2010) 217–223. doi:10.1016/j.biopsych.2009.08.005. [PubMed: 19782964]

[68]. Lim YH, Lee HC, Falkmer T, Allison GT, Tan T, Lee WL, Morris SL, Effect of Visual Information on Postural Control in Adults with Autism Spectrum Disorder, J. Autism Dev. Disord (2018). doi:10.1007/s10803-018-3634-6.

[69]. Marko MK, Crocetti D, Hulst T, Donchin O, Shadmehr R, Mostofsky SH, Behavioural and neural basis of anomalous motor learning in children with autism, Brain. 138 (2015) 784–797. doi:10.1093/brain/awu394. [PubMed: 25609685]

[70]. Minshew NJ, Sung K, Jones BL, Furman JM, Underdevelopment of the postural control system in autism, Neurology. 63 (2004) 2056–2061. doi:10.1212/01.WNL.0000145771.98657.62. [PubMed: 15596750]

[71]. Kent JS, Hong SL, Bolbecker AR, Klaunig MJ, Forsyth JK, O'Donnell BF, Hetrick WP, Motor Deficits in Schizophrenia Quantified by Nonlinear Analysis of Postural Sway, PLoS ONE. 7 (2012) e41808. doi:10.1371/journal.pone.0041808. [PubMed: 22870250]

[72]. Spencer AH, Rickards H, Fasano A, Cavanna AE, The prevalence and clinical characteristics of punding in Parkinson's disease: Punding in Parkinson's Disease, Mov. Disord 26 (2011) 578–586. doi:10.1002/mds.23508. [PubMed: 21648123]

[73]. Morrens M, Hulstijn W, Lewi PJ, De Hert M, Sabbe BGC, Stereotypy in schizophrenia, Schizophr. Res 84 (2006) 397–404. doi:10.1016/j.schres.2006.01.024. [PubMed: 16549339]

[74]. American Psychiatric Association, Diagnostic and statistical manual of mental disorders (DSM-5®), American Psychiatric Publishing, Arlington, VA, 2013.

[75]. Goldman S, Wang C, Salgado MW, Greene PE, Kim M, Rapin I, Motor stereotypies in children with autism and other developmental disorders, Dev. Med. Child Neurol 51 (2009) 30–38.

[76]. Newell KM, Broderick MP, Deutsch KM, Slifkin AB, Task goals and change in dynamical degrees of freedom with motor learning., J. Exp. Psychol. Hum. Percept. Perform 29 (2003) 379–387. doi:10.1037/0096-1523.29.2.379. [PubMed: 12760622]

[77]. Grundy JG, Barker RM, Anderson JAE, Shedden JM, The relation between brain signal complexity and task difficulty on an executive function task, NeuroImage. 198 (2019) 104–113. doi:10.1016/j.neuroimage.2019.05.045. [PubMed: 31112787]

[78]. Szostakiwskyj JMH, Willatt SE, Cortese F, Protzner AB, The modulation of EEG variability between internally- and externally-driven cognitive states varies with maturation and task performance, PLOS ONE. 12 (2017) e0181894. doi:10.1371/journal.pone.0181894. [PubMed: 28750035]

Highlights

- Accuracy of precision movements improves with visual feedback
- Complexity of precision movements increases in the presence of visual feedback
- Visual feedback increases the complexity of sensorimotor neural signals
- Increased visual-motor integration corresponds with more adaptive motor output

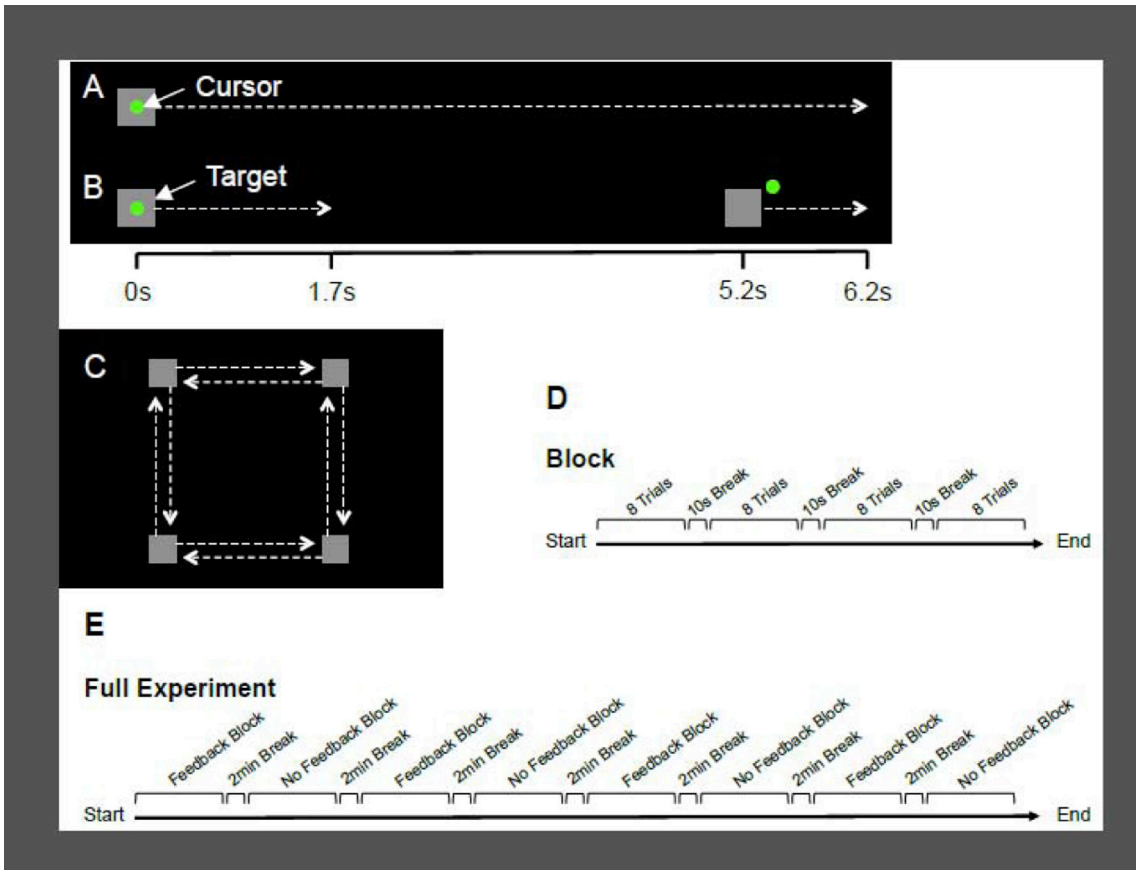

Figure 1. Task Design.

A) Depiction of a Feedback trial with the target in grey and the cursor in green. The target and cursor are visible for the entire duration of the trial. **B)** Depiction of a No Feedback trial. The target and cursor disappear 1.7s after the target starts moving. They are invisible for 3.5s before reappearing at the end of the trial**. C)** Trials can start at any one of four locations and move in any of four directions. **D)** Structure of a block of trials. All trials within a block are the same sensory feedback condition. **E)** Structure of the task. Blocks alternate between Feedback and No Feedback. The condition of the starting block is randomly decided for each participant.

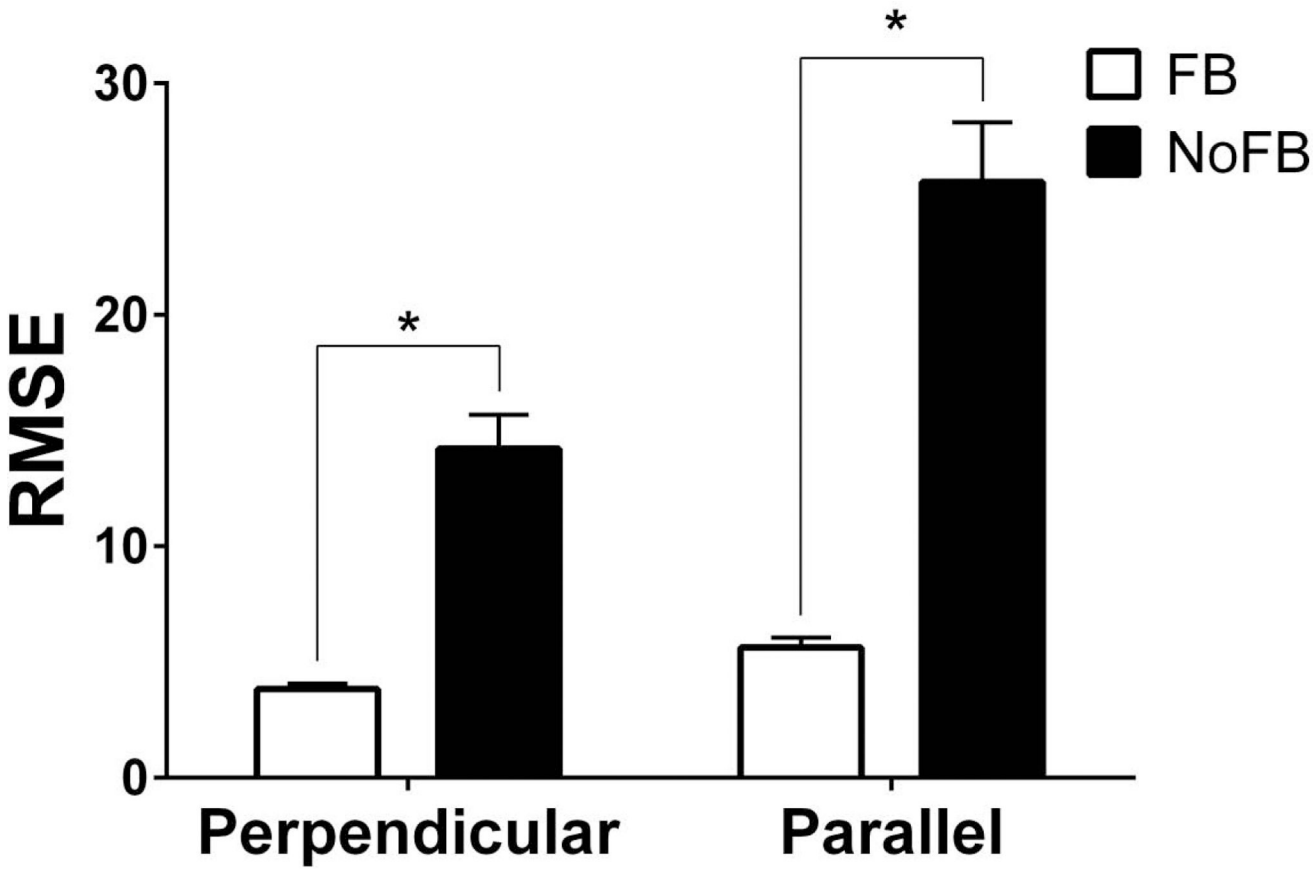

Figure 2. Motor Performance.

Performance was measured using the root mean square error (RMSE) of the cursor position relative to the target. Higher values represent poorer performance. Error is indicated for the perpendicular axis of motion (left) and parallel axis of motion (right) for the Feedback condition (white) and the No Feedback condition (black). Significant differences between feedback conditions are indicated by *. Error bars represent standard error of the mean.

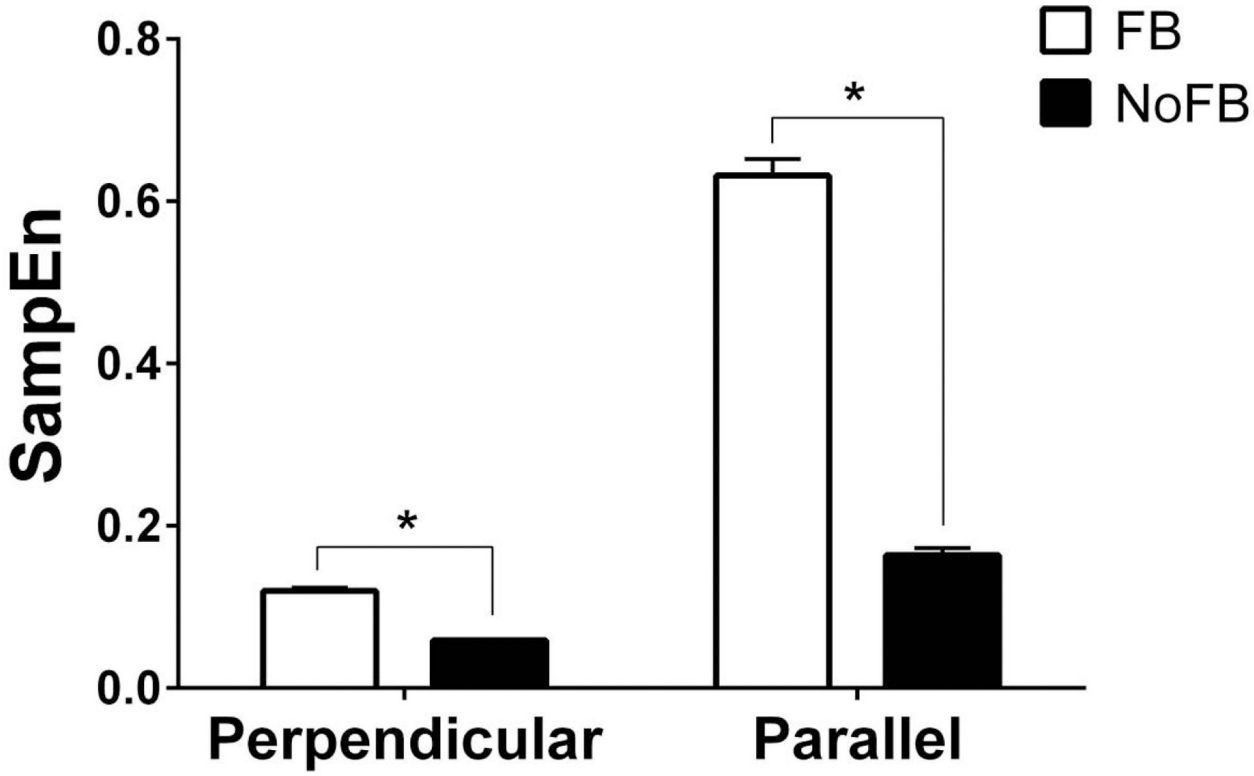

Figure 3. Motor Complexity.

Motor complexity on the task was calculated using sample entropy (SampEn) of the time series of the cursor position relative to the target. Motor complexity is indicated for the perpendicular axis of motion (left) and parallel axis of motion (right) for the Feedback condition (white) and the No Feedback condition (black). Significant differences between feedback conditions are indicated by *. Error bars represent standard error of the mean.

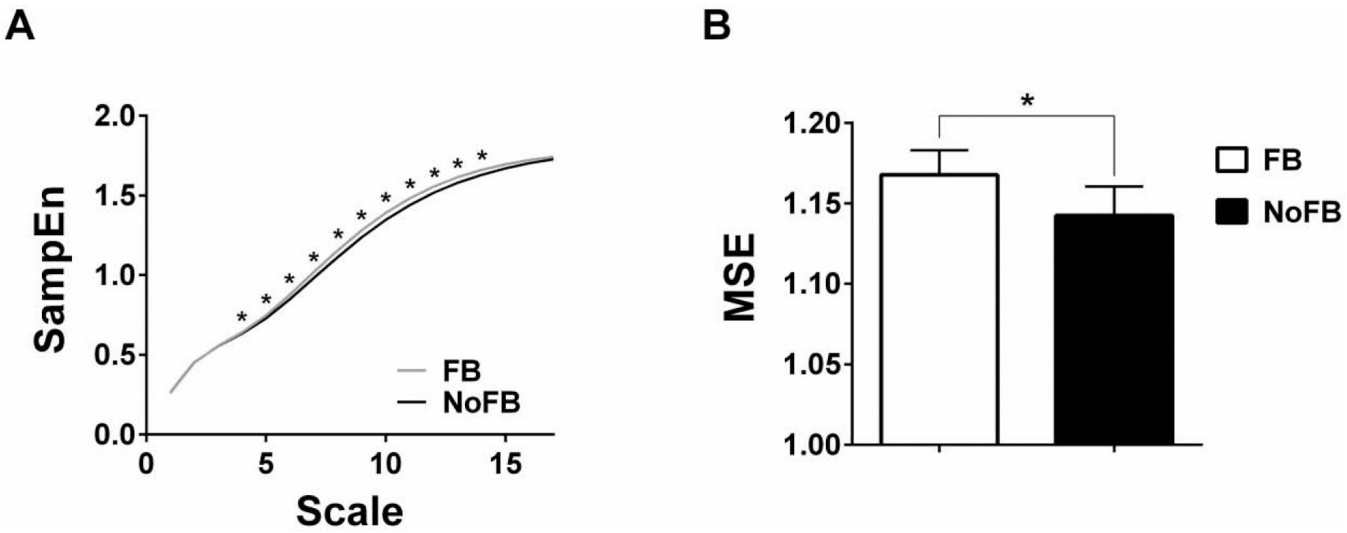

Figure 4. Overall Neural Complexity.

A) Sample entropy (SampEn) averaged across all electrodes for each time scale for each sensory feedback condition (Feedback: grey circles, No Feedback: black squares). Time scales for which the Feedback and No Feedback conditions significantly differed are indicated by *. **B)** Multi-scale Sample Entropy (MSE) values calculated by averaging across all electrodes and all time scales for each sensory feedback condition (Feedback: white, No Feedback: black). The significant difference between sensory feedback conditions is indicated by *. Error bars represent standard error of the mean.

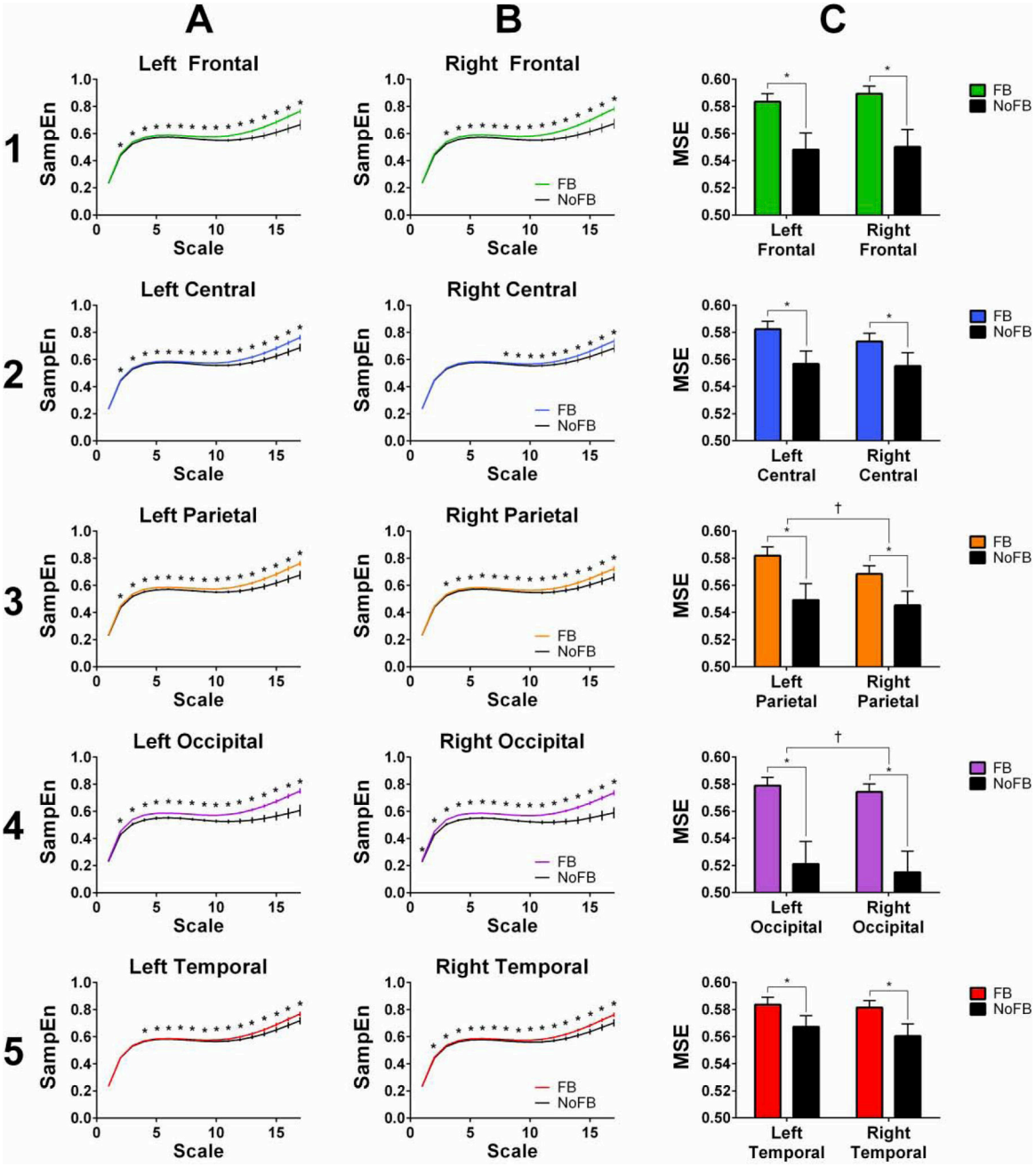

Figure 5. Alpha Band Neural Complexity by Scalp Region.

Alpha band neural complexity during the task was calculated using multi-scale sample entropy (MSE). Rows (numbered) indicate different scalp regions: **1)** Frontal, **2)** Central, **3)** Occipital, **4)** Temporal. Columns **A** and **B** depict the neural complexity (SampEn) at each time scale for the left and right hemispheres, respectively. Time scales for which the neural complexity differed significantly between the Feedback condition (colored circles) and the No Feedback condition (black squares) are indicated by *. Column **C** represents the across-scales average for each scalp region and sensory feedback condition. Significant differences between the Feedback condition (colored bars) and No Feedback condition (black bars) are

indicated by *. Significant differences between activity in Left and Right hemisphere are indicated by † Error bars represent standard error of the mean.

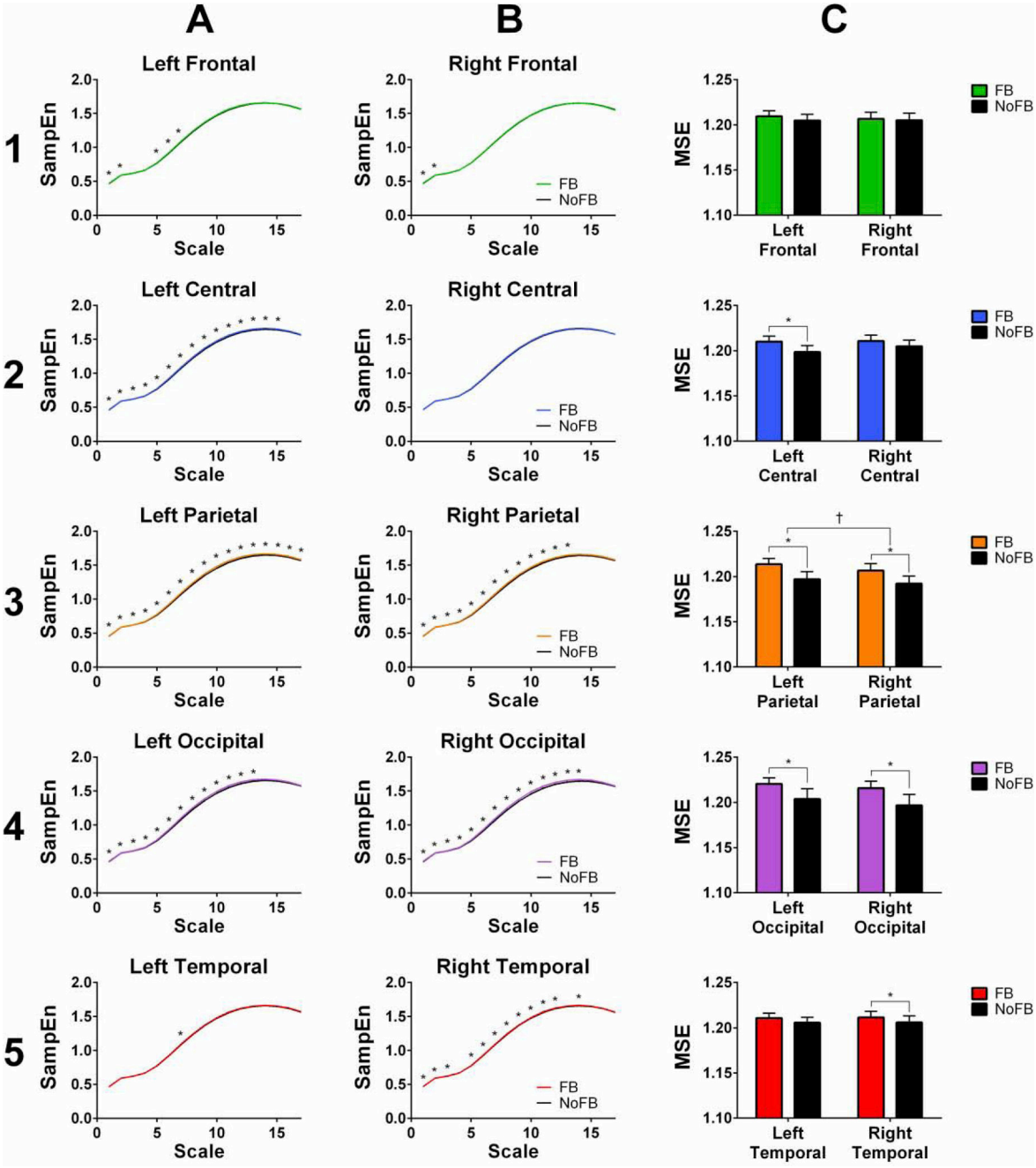

Figure 6. Beta Band Neural Complexity by Scalp Region.

Beta band neural complexity during the task was calculated using multi-scale sample entropy (MSE). Rows (numbered) indicate different scalp regions: **1)** Frontal, **2)** Central, **3)** Occipital, **4)** Temporal. Columns **A** and **B** depict the neural complexity (SampEn) at each time scale for the left and right hemispheres, respectively. Time scales for which the neural complexity differed significantly between the Feedback condition (colored circles) and the No Feedback condition (black squares) are indicated by *. Column **C** represents the across-scales average for each scalp region and sensory feedback condition. Significant differences between the Feedback condition (colored bars) and No Feedback condition (black bars) are

indicated by *. Significant differences between activity in Left and Right hemisphere are indicated by † Error bars represent standard error of the mean.

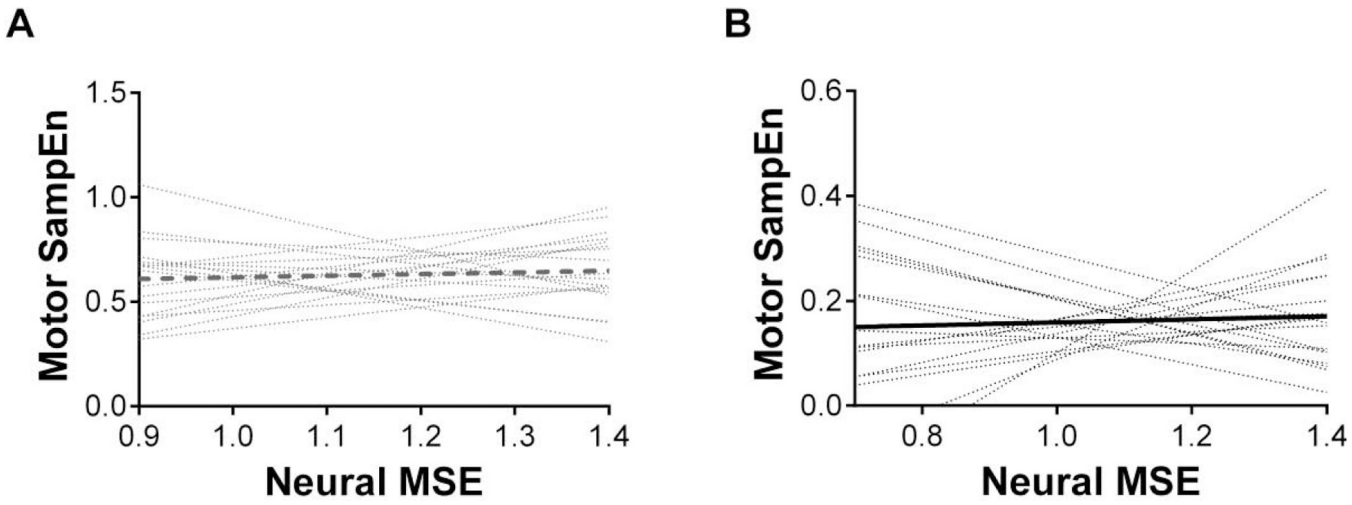

Figure 7. Relation between Motor (SampEn) and Neural (MSE) Complexity.

A) Individual participant (thin dotted lines) and average slope (thick dashed line) in the Feedback condition (grey), **B)** Individual participant (thin dotted lines) and average slope (thick solid line) in the No Feedback condition (black).